

Light Water Reactor Sustainability Program

Dielectric Spectroscopy for Bulk Condition Assessment of Cable Insulation



September 2019

U.S. Department of Energy

Office of Nuclear Energy

DISCLAIMER

This information was prepared as an account of work sponsored by an agency of the U.S. Government. Neither the U.S. Government nor any agency thereof, nor any of their employees, makes any warranty, expressed or implied, or assumes any legal liability or responsibility for the accuracy, completeness, or usefulness, of any information, apparatus, product, or process disclosed, or represents that its use would not infringe privately owned rights. References herein to any specific commercial product, process, or service by trade name, trade mark, manufacturer, or otherwise, does not necessarily constitute or imply its endorsement, recommendation, or favoring by the U.S. Government or any agency thereof. The views and opinions of authors expressed herein do not necessarily state or reflect those of the U.S. Government or any agency thereof.

Dielectric Spectroscopy for Bulk Condition Assessment of Cable Insulation

**Authors: S.W. Glass¹, L.S. Fifield¹, N. Bowler²,
A. Sriraman², C. Gifford²**

**¹Pacific Northwest National Laboratory
²Iowa State University**

September 2019

**Prepared for the
U.S. Department of Energy
Office of Nuclear Energy**

Light Water Reactor Sustainability Program

**Dielectric Spectroscopy for Bulk Condition
Assessment of Cable Insulation**

PNNL-29092

September 2019

Approved by:

Gertrude Patello

Gertrude Patello, Director
Nuclear Science Project Management Office

September 11, 2019

Date

SUMMARY

This Pacific Northwest National Laboratory milestone report describes progress to date on the investigation of nondestructive test methods focusing on bulk cable insulation testing using a dielectric spectroscopy (DS) approach. This report addresses relevant literature coupled with a discussion of the theory of DS measurements and work on modeling to appreciate the influence of damage/defect profile on the bulk total cable measurement.

A twisted shielded triplex ethylene propylene rubber (EPR) cable with a well-aged segment as part of the total cable was tested for its DS measuring capacitance and dissipation factor. The percentage of aged cable compared to the total sample length is designated as the damage ratio (R). The capacitance (C) was presented as specific capacitance (pF/m), i.e., normalized by length. As R was increased from 3% to 90%, the specific capacitance is observed to increase from 190 to 250 pF/m or 32% and the dissipation factor (D) increased from 0.0034 to 0.0051 or approximately 50%.

Conclusions and observations are as follows:

- A substantial body of work suggests feasibility to measure cable insulation conditions using various forms of DS.
- Measured specific C and D
 - 1) increases significantly with thermal aging of flame-resistant EPR/chlorinated polyethylene shielded triad instrumentation cable (General Cable) due to material property changes
 - 2) increases linearly with increasing damage ratio, R, in a cable.
- Specific C
 - 1) decreases linearly with increasing area of removed cable jacket and/or shield
 - 2) C decreases to a relatively larger degree when both jacket and shield are removed.
- The thermally aged section of the cable significantly increases capacitance values even at low R.
- D shows the same increasing trend with R and to a relatively larger degree.
- The DS measurement represents an average of the dielectric condition over the entire cable. If only a small percentage of the cable is damaged, this should be considered when assessing the DS measurement. An assumption that the damage is distributed along the entire cable length is a non-conservative assumption.

ACKNOWLEDGMENTS

This research was sponsored by the U.S. Department of Energy, Office of Nuclear Energy, for the Light Water Reactor Sustainability (LWRS) Program Materials Research Pathway. The authors extend their appreciation to Dr. Thomas Rosseel for LWRS programmatic support.

Pacific Northwest National Laboratory (PNNL) is operated by Battelle Memorial Institute for the U.S. Department of Energy under Contract No. DE-AC05-76RL01830.

The work performed by Iowa State University was performed under a subcontract from PNNL.

Contributions from University of Bologna are part of the 2017 U.S.-EURATOM International Nuclear Energy Research Initiative (INERI), “Advanced Electrical Methods for Cable Lifetime Management” project with PNNL.

CONTENTS

SUMMARY	iii
ACKNOWLEDGMENTS	iv
CONTENTS.....	v
FIGURES.....	vii
TABLES	vii
ACRONYMS AND ABBREVIATIONS	viii
1. OBJECTIVES.....	1
2. BACKGROUND AND LITERATURE REVIEW	2
2.1 EPRI Technical Report 105581: Improved Conventional Testing of Power Plant Cables.....	2
2.2 U.S. NRC Report NUREG/CR-6904: Evaluation of the Broadband Impedance Spectroscopy Prognostic/Diagnostic Technique for Electric Cables Used in Nuclear Power Plants.....	3
2.3 European ADVANCE – Ageing Diagnostics and Prognostics of Low-Voltage I&C Cables – Project 269983	3
2.4 IAEA Coordinated Research Project Condition Monitoring and Management of Ageing of Low Voltage Cables in Nuclear Power Plants	4
2.5 EPRI Technical Report 3002010403: Long-Term Operations: Initial Findings on Use of Dielectric Spectroscopy for Condition Monitoring of Low Voltage Nuclear Power Plant Cables	5
2.6 Dielectric Spectroscopy for Diagnostics of Water Tree Deteriorated XLPE Cables.....	5
2.7 Dielectric Spectroscopy as a Condition Monitoring Technique for Cable Insulation Based on Cross-linked Polyethylene.....	5
2.8 Dielectric Spectroscopy as a Condition Monitoring Diagnostic Technique for Thermally Aged PVC/EPR Nuclear Power Plant Cables	6
2.9 Submerged Medium Voltage Cable Systems at Nuclear Power Plants: A Review of Research Efforts Relevant to Aging Mechanisms and Condition Monitoring.....	6
3. DIELECTRIC SPECTROSCOPY THEORY	7
3.1 Parallel Plate Capacitor to Measure Dielectric Coefficient	7
3.2 Permittivity of Polymers	8
3.3 Cable System Capacitance and Impedance.....	9
4. DS MEASUREMENTS ON TRIPLEX (THREE-CONDUCTOR) CABLE.....	11
4.1 Cable Sample Preparation.....	11
4.1.1 Cable	11
4.1.2 Samples.....	12
4.2 DS Measurement Method	13
4.2.1 Experiment Procedure.....	13

4.2.2	Experiment Sequence.....	13
4.3	Results and Discussion.....	14
5.	CONCLUSIONS	20
6.	PLANS FOR CONTINUED WORK	21
7.	REFERENCES	22

FIGURES

Figure 3.1.	Parallel capacitor model with dielectric sandwiched between two conductive plates.....	7
Figure 3.2.	Frequency-dependence of ϵ' and ϵ'' for relaxation modes in typical polymers (Bowler and Liu 2015).....	8
Figure 3.3.	Configuration and formulas for calculating nominal cable capacitance (Standard Wire & Cable Co. 2009).....	9
Figure 3.4.	Simulated magnitude Z (ohms) plot of pristine, 50% aged, and 100% aged twisted-pair cable based on simple resistance and capacitance series and parallel impedance model.	10
Figure 4.1.	Cross-section schematic of the cable (<i>left</i>) and photograph (<i>right</i>).....	11
Figure 4.2.	Pristine samples with length 9.5 cm (a), 47.7 cm (b), and 308 cm (c).	12
Figure 4.3.	Cable with aged section: aging setup (<i>left</i>) and photograph of the aged cable section showing loss of jacket and shield in places (<i>center</i> and <i>right</i>). Grid is 1 cm.	12
Figure 4.4.	Agilent two-point 16095A probe test fixture in contact with cable sample.....	13
Figure 4.5.	Absolute capacitance measured on pristine samples.	14
Figure 4.6.	Insulation real relative permittivity inferred from capacitance data shown in Figure 4.5, measured on pristine samples of different length, by COMSOL™ simulation.	15
Figure 4.7.	Specific capacitance (distributed) measured on samples with various values of R.....	16
Figure 4.8.	Dissipation factor (distributed) measured on samples with varying values of R.....	16
Figure 4.9.	Specific capacitance measured on samples with various lengths (Table 4-3) plotted as a function of distance from aged cable section.....	17
Figure 4.10.	Dissipation factor measured on samples with various lengths (Table 4-3) plotted as a function of distance from the aged cable section.....	18
Figure 4.11.	Specific capacitance (distributed) measured on pristine samples with various lengths plotted as a function of sample (segment) length for frequency 1.02 kHz.	18
Figure 4.12.	Dissipation factor measured on pristine samples with various lengths plotted as a function of sample (segment) length for frequency 1.02 kHz.	19
Figure 4.13.	Specific capacitance (distributed) measured on 100 cm long pristine samples as a function of the length of removed jacket or jacket and shield.....	19

TABLES

Table 4-1.	Cable dimensions.....	11
Table 4-2.	Sample specifications.	12
Table 4-3.	Sample section lengths, aged cable. Samples AP1 and AP8 were at each end of the original cable; whereas, AP7 and AP14 were adjacent to the aged section, as in the order listed in the table.	14

ACRONYMS AND ABBREVIATIONS

AMP	aging management program
AWG	American wire gauge for diameters of round, solid, electrically conductive wire
C	capacitance
CPE	chlorinated polyethylene
δ	penetration depth
DBE	design basis event
D	dissipation factor (dimensionless) also referred to as Tan Delta
DC	direct current
DS	dielectric spectroscopy
ε	complex permittivity
EAB	elongation at break
EPR	ethylene propylene rubber
EPRI	Electric Power Research Institute
f	frequency
F	SI unit of capacitance
FDR	frequency domain reflectometry
ft.	foot (12 inches)
FTIR	Fourier-transform infrared spectroscopy
IAEA	International Atomic Energy Agency
LCR	inductance-capacitance-resistance
LFDS	low frequency dielectric spectroscopy
LOCA	loss-of-coolant accident
LV	low voltage
LWRS	Light Water Reactor Sustainability Program
NDE	nondestructive evaluation
NPP	nuclear power plant
PDC	polarization/depolarization current
pF	pico Farad
PNNL	Pacific Northwest National Laboratory
PVC	polyvinyl chloride
R	damage ratio
sf	stranding factor
tan delta (δ)	dissipation factor
XLPE	cross-linked polyethylene

1. OBJECTIVES

This Pacific Northwest National Laboratory (PNNL) milestone report describes progress to date on the investigation of nondestructive test methods focusing particularly on dielectric spectroscopy (DS) testing of cable that provide key indication of cable aging and damage.

An overall objective of this program is to develop the technical basis for assessing the level and impact of cable insulation aging and degradation in nuclear power plants (NPPs). In July 2012, a workshop (Simmons et al. 2012) was held to lay the groundwork for a research and development roadmap to address aging cable management in NPPs, including methods for nondestructively measuring the condition of aging cables. The program addresses the overall gaps that were identified at that workshop using a phased approach. This phased approach addresses the three areas identified from the workshop:

1. Determine key indicators of cable aging. This has largely been addressed in earlier reports (Simmons et al. 2014; Fifield et al. 2015; Ramuhalli et al. 2015).
2. Characterize and advance current nondestructive evaluation (NDE) methods and develop new NDE methods by using insights from the determination of key indicators. This activity was generally addressed by Glass et al. (2015) describing the overall state of the art for both bulk electrical tests and local tests. More focused reports have been prepared to address local NDE cable tests (Glass et al. 2016); bulk and distributed cable tests, particularly focusing on frequency domain reflectometry (Glass et al. 2017), and interdigital capacitance (Glass et al. 2018a). This 2019 report continues efforts to characterize and advance NDE methods, focusing on DS initiated in Glass et al. (2018a); Glass et al. (2018b)).
3. Develop models that use the advances in identification of key indicators and NDE methods to help predict the remaining life of cables. Modeling has been and continues to be essential to understanding the relevance and aid in the interpretation of NDE results. Examples of this include Glass et al. (2016); Glass et al. (2018a); Glass et al. (2018b), as well as this report on DS.

This report is submitted in fulfillment of deliverable M4LW-19OR0404025–Report on Dielectric Spectroscopy (DS) Assessment of Aging Cable Insulation for Nuclear Power Plant Cable Aging Management Programs.

2. BACKGROUND AND LITERATURE REVIEW

As NPPs apply for a second or subsequent license renewal to extend their operating period from 60 to 80 years, it is important to understand how materials installed in plant systems and components will age during that time and develop aging management programs (AMPs) to assure continued safe operation under normal and design-basis events (DBEs). Degradation of cable insulation is known to occur as a function of age, temperature, radiation, and other environmental factors. Although system tests verify cable function under normal loads, concerns remain over cable performance under exceptional loads associated with DBEs. The cable's ability to perform safely over the initial 40-year planned and licensed life has generally been demonstrated, and there have been very few age-related cable failures (EPRI 2015; Mantey 2015). With greater than 1000 km of power, control, instrumentation, and other cables typically found in an NPP, replacing all the cables would be a severe cost burden. License renewal to 60 years and subsequent license renewal to 80 years, therefore, requires a cable AMP in accordance with regulatory guidance (NRC 2012) to justify cable performance under normal operation as well as accident conditions.

Acceptance criteria that define the threshold for degradation below which cables may continue to be used are a challenge, because it is impractical to subject each cable system to loss-of-coolant accident (LOCA) or seismic simulation events following 40+ years of service. The report *Initial Acceptance Criteria Concepts and Data for Assessing Longevity of Low-Voltage Cable Insulations and Jackets* (EPRI 2005) develops a basis for acceptance criteria and evaluates the aging profiles for many commonly used cable jackets and polymers. The report describes 50% elongation at break (EAB) as a conservative practical end-of-life threshold for cables that may be stressed during maintenance or subjected to LOCA exposure. The report also discusses the basis for cautious continued use of cables beyond the 50% EAB threshold. EAB inherently compromises the in-service cable use as it is a destructive ex situ test, so the challenge is to develop NDE methods that can reasonably be correlated with EAB. Reliable NDE in situ approaches are needed to objectively determine the suitability of installed cables for continued service. A variety of tests are available to assess various aspects of electrical and mechanical cable performance, but none of the available tests are suitable for all cable configurations nor does any single test assess all features of interest. DC withstand tests at or above the rated cable voltage and low frequency tan delta (δ) tests are widely applied, particularly during installation to confirm quality installations, but these tests should not be used excessively as they do stress the polymers and may reduce the life of the cable system.

Low-voltage DS has been used for decades to characterize the electrical behavior of polymers and other dielectric materials without introducing any significant damage to the dielectric material (Kremer and Schonhals 2003). Several researchers have applied this general method to cable tests as indicated below.

2.1 EPRI Technical Report 105581: Improved Conventional Testing of Power Plant Cables

Toman (2011) lists and describes the state of the art for in situ nuclear plant cable tests and characterizes advantages and weaknesses of each test, with particular focus on aged unshielded power cables for instrumentation and control (600V–5kV) from Canadian nuclear and thermal generation plants. This report describes a DS test as a current passing through the insulation in response to a step change in voltage that is analyzed by transforming the acquired current data into a function of frequency to arrive at dielectric impedance as a function of frequency. The variation in dielectric impedance is primarily due to bulk cable capacitance and conductance. The real and imaginary parts of the permittivity, the change in the real permittivity, and the $\tan \delta$ are evaluated with respect to voltage and frequency change. At each applied voltage, a frequency sweep is performed, and the permittivity and $\tan \delta$ parameters are evaluated.

The following four behaviors have been defined:

- Low-loss, linear permittivity: The response for new or non-water tree deteriorated cables. The results are nearly frequency-independent, the loss is low and has a very weak frequency dependence, and the real and imaginary parts of the permittivity are independent of applied voltage.
- Voltage-dependent permittivity: An indication of water treeing that is significant but has not yet penetrated the whole of the insulation, in which the real and imaginary parts of the permittivity are voltage-dependent.
- Transition to leakage current: An indication that the water trees penetrate through the wall of the insulation and that the breakdown strength of the insulation is significantly reduced. The transition is indicated by an increased loss at the time of applied voltage. In other words, the second measurement at a specific voltage level has a higher loss than the initial measurement.
- Leakage current: An indication that water trees penetrate the whole of the insulation and the cable has very low breakdown strength. Leakage current is observed at low voltages, loss increases with decreasing frequency, and the real part of the permittivity shows a voltage-dependent response.

The study concluded that none of the conventional diagnostic measurements (DC insulation resistance, polarization index, high-voltage partial discharge, capacitance, dissipation factor) used were sensitive to unshielded cable degradation. Moreover, the value of testing at frequencies other than power frequencies was highlighted.

2.2 U.S. NRC Report NUREG/CR-6904: Evaluation of the Broadband Impedance Spectroscopy Prognostic/Diagnostic Technique for Electric Cables Used in Nuclear Power Plants

Rogovin and Lofaro (2006) focused on the application of broadband impedance spectroscopy as a condition monitoring tool for low-voltage (LV) instrumentation and control (I&C) cables found in NPPs. Samples of a two-conductor I&C cable were subjected to thermal aging over their entire length or at discrete locations to simulate the effect of hot spots. The resulting sample population included cables with different levels of aging, ranging in size from 10 m to 100 m. The presence of mechanical defects, such as abrasion and racks, was also investigated. Samples were tested with a broadband impedance analyzer over a frequency range of 100 Hz to 100 MHz. Impedance magnitude and phase were extracted from the complex impedance spectra to determine the sensitivity of the method to thermal aging. Analytical models were developed to simulate the test response and interpret the experimental data. The technique was found to be sensitive to global thermal aging in the frequency range below 1 MHz, with the measured impedance phase spectra showing an increase in the impedance phase angle for higher levels of aging. In the frequency range above 1 MHz, the impedance magnitude and phase spectra were downshifted to lower frequencies with increasing level of aging. These findings indicated that the method could be used as an indicator of thermal degradation on the cable.

2.3 European ADVANCE – Ageing Diagnostics and Prognostics of Low-Voltage I&C Cables – Project 269983

The ADVANCE project (European Commission 2014) was a European-led collaborative project involving a number of industrial, research, and academic partners. The main objectives of the project were to assess and optimize promising nondestructive condition monitoring methods to assess the condition of safety-related LV cables over their entire length and to develop acceptance criteria for these methods.

The first stage of the project established the potential application of state of the art of condition monitoring methods for LV cables in NPPs. The research looked at the advantages and disadvantages of laboratory and field techniques based on the physical/mechanical characterization of cable insulation and

jacket materials. The use of electrical techniques was also investigated, and it was concluded that information about the effect of aging on electrical properties of LV cable insulation is still lacking. Based on this information a research program was developed to investigate and improve the most promising techniques. The program included long and short cable samples subjected to combined thermal and radiation aging and characterized at regular intervals with selected condition monitoring methods. The long cable samples also went through design basis accident testing to correlate condition indicators measured near the cable end of life with cable survivability.

No single condition monitoring method was shown to be sufficient to track degradation at all stages; hence, it was recommended to use a combination of techniques until aging mechanisms are sufficiently identified. From tests on longer samples (i.e., about 20 m), no general behavior was observed; i.e., it was hypothesized that each cable type (or group) may require the most appropriate condition monitoring method/marker to be defined or at least tuned. Among electrical techniques investigated in the work, low-frequency dielectric spectroscopy (LFDS) (obtained using frequency domain techniques) showed the most promising results. In particular, between 10^{-2} Hz and $\sim 10^6$ Hz, test results on short samples showed that both real (a') and imaginary (a'') parts of permittivity of cross-linked polyethylene (XLPE), ethylene propylene rubber (EPR)-based, and ethylene propylene diene monomer (EPDM) rubber-based insulations increased over the whole frequency range. The variation of a' was more evident at low frequency, while a'' increased markedly also in the high-frequency range. The change in electrical properties appeared to correlate well with traditional material-based characterization techniques.

Other techniques such as frequency domain reflectometry (FDR) were noted to be able to locate hot-spots or locations for the greatest potential for damage. Defect location is not provided by DS measurements. The importance of measurement technique and environmental controls, particularly of temperature, were also noted.

2.4 IAEA Coordinated Research Project Condition Monitoring and Management of Ageing of Low Voltage Cables in Nuclear Power Plants

The intent of this large collaborative project (IAEA 2017) between 17 participating countries was to provide comprehensive information and guidelines on how to monitor the condition of LV cables in NPPs. To achieve this goal, a benchmarking program was established to assess well-established and new condition monitoring techniques on cables exposed to accelerated thermal and radiation aging. There were 14 different methods, material-based and electrical, used to test 12 different types of cables. The various participants used the selected methods, and results were compared to determine their respective efficacy and accuracy to measure the level of aging for each cable. Among the material-based techniques, EAB and indenter modulus were found to be the most sensitive to degradation as a result of aging for most materials. Oxidation induction time and oxidation induction temperature also yielded trendable results for a number of cable formulations. Fourier-transform infrared spectroscopy (FTIR), ultrasonic velocity, and density were found to be promising in the early stage of aging and have some trendable potential for some materials.

LFDS and FDR were found to be the only electrical tests with the potential to trend the degradation of the insulation materials. While FDR was determined to be most useful to detect local areas of degradation, LFDS was found to be able to track changes in the bulk properties of the insulation, more so for irradiated samples than for thermally aged samples. The LFDS tests were conducted between 10^{-2} and 10^6 Hz on short cable samples (up to 1 m) by the University of Bologna. The measurements were made between individual wires or between shield and individual wires for shielded cables. Only a few cables were tested as part of this work, but the influence of stray capacitances on the repeatability of results for unshielded cables was noted. It was also reported that testing at higher temperatures enhances the sensitivity of the method to detect material degradation induced by aging.

2.5 EPRI Technical Report 3002010403: Long-Term Operations: Initial Findings on Use of Dielectric Spectroscopy for Condition Monitoring of Low Voltage Nuclear Power Plant Cables

The Electric Power Research Institute (EPRI 2017) sought to address the question: Is there a diagnostic test that can be applied to a wide range of LV cable insulation types and configurations that provide a global indication of thermal degradation of a cable circuit whether it is shielded or unshielded? The research applied LFDS and polarization/depolarization current (PDC) methods that focused on both time-domain (for very low frequencies [0.01–10 Hz]) and frequency domain (for >10 Hz) methods to assess thermal aging effects on several cables, including:

- a 3-conductor control cable
- a 3-conductor power cable
- a conductor instrument and control cable.

DS tests were performed in various configurations (electrode grounding, external mandrel grounding, applied voltage level, ambient temperature, etc.) and were compared to common physical and chemical cable aging tests of indenter modulus, EAB, near infrared, infrared (FTIR), etc. Key findings included the following:

- LFDS and PDC measurements can be sensitive enough to detect bulk thermal aging effects (e.g., structural changes in polymer, depletion of antioxidants) in a variety of shielded and unshielded LV cable insulation types and geometric configurations.
- A variety of diagnostic “metrics” derived from the variable frequency and time-dependent dielectric response data showed quantifiable trends versus increasing levels of thermal aging. The trends varied depending on the analyzed parameter and with temperature.
- Experimental parameters and test configurations specific to the cable under test must be carefully considered to obtain optimal dielectric response measurement data.
- The results from the study highlighted the unique (cable-specific) and frequency and time-dependent dielectric response characteristics of LV multi-conductor cables with different insulation types to bulk thermal aging.

2.6 Dielectric Spectroscopy for Diagnostics of Water Tree Deteriorated XLPE Cables

A high-voltage DS system was developed under Werelius et al. (2001) for diagnosis of water tree-deteriorated extruded medium-voltage cable based on measurements of non-linear dielectric response in the frequency domain to measure relatively low loss and small variations of permittivity as a function of frequency and voltage. Experience from more than 200 field measurements was combined with laboratory investigations of accelerated aged samples. The dielectric response of water tree-deteriorated XLPE cables was shown to correlate with aging and breakdown strength. Two different field studies of implementation of this diagnostic method were also presented. The field studies showed the fault rate decreased significantly when replacement strategy was based on the diagnostic criteria formulated.

2.7 Dielectric Spectroscopy as a Condition Monitoring Technique for Cable Insulation Based on Cross-linked Polyethylene

Linde et al. (2015) evaluated DS as a condition monitoring technique for aged XLPE electrical insulation in NPPs. Bare core XLPE samples were aged at 55°C and 85°C and under exposure to ⁶⁰Co γ -radiation at different dose rates (0.42–1.06 kGy h⁻¹). Samples were assessed using a variety of methods including DS, tensile testing, crystallinity, density, and FTIR. Results suggest that DS can be used for in

situ measurements of the degree of oxidation of XLPE cables in order to assess cable condition and remaining useful life.

2.8 Dielectric Spectroscopy as a Condition Monitoring Diagnostic Technique for Thermally Aged PVC/EPR Nuclear Power Plant Cables

Imperatore (2017) examined LV DS responses of polyvinyl chloride (PVC)/EPR multi-conductor cables aged at PNNL compared to EAB and other cable condition metrics. Specific capacitance and dissipation factor measurements showed a monotonic trend that correlated well with aging at 10 Hz, 1 kHz, and 100 kHz. For these samples, the 1 kHz response was the best DS diagnostic marker. The DS change preceded any significant change in EAB, thereby indicating that this measurement could be an earlier indicator of the onset of damage than mechanical measurements.

2.9 Submerged Medium Voltage Cable Systems at Nuclear Power Plants: A Review of Research Efforts Relevant to Aging Mechanisms and Condition Monitoring

Brown et al. (2015) examined various test approaches being applied to nuclear plant submerged medium-voltage cables. This work included discussions of damage mechanisms and how test stresses interact with water-tree and other insulation flaws. One observation noted that the length of a stressed cable section may be quite small compared to the total cable length being tested. The example identified a 1-meter stressed cable section in a 1-kilometer cable representing 0.1% of the total cable length. Many bulk condition monitoring tests, including $\tan \delta$ and PDC tests consider the bulk cable condition. Test sensitivities must be high to detect damage affecting such a small portion of the object under test.

3. DIELECTRIC SPECTROSCOPY THEORY

3.1 Parallel Plate Capacitor to Measure Dielectric Coefficient

The simplest form of a DS measurement is the characterization of the electrical impedance of a parallel plate capacitor. Capacitive sensors are used in the area of materials characterization known as *dielectrometry* (Nassr and El-Dakhkhni 2009; Sheldon and Bowler 2014a). The output capacitance of a capacitive sensor placed in the vicinity of a test material is sensitive to the dielectric properties of that material. Capacitance can be measured using a typical inductance-capacitance-resistance (LCR) meter connected to a capacitive probe.

Generally familiar is the parallel plate capacitor configuration with a dielectric wafer sandwiched between charged (+/-Q) conductive plates (Figure 3.1) whose complex capacitance C^* (F) is given by

$$C^*(f) = \varepsilon^*(f) A/d$$

where

$$\varepsilon^* = \varepsilon' - j\varepsilon'' \text{ [F/m]} = \text{complex permittivity of the material that fills the space between the capacitor plates,}$$

$$A \text{ [m}^2\text{]} = \text{area of one of the two identical capacitor electrodes,}$$

$$d \text{ [m]} = \text{uniform separation between them, and}$$

$$f \text{ [Hz]} = \text{frequency.}$$

Parallel-plate electrodes are suitable for dielectrometry on flat specimens of uniform thickness that are somewhat thinner than the diameter of the electrodes and can be accessed on both sides. For other sample shapes, and in the case of samples that can be accessed from only one side, custom capacitive electrodes can be designed according to various considerations (Chen and Bowler 2009; Chen and Bowler 2013; Sheldon and Bowler 2014b). These design considerations usually involve a trade-off between signal amplitude and sensitivity.

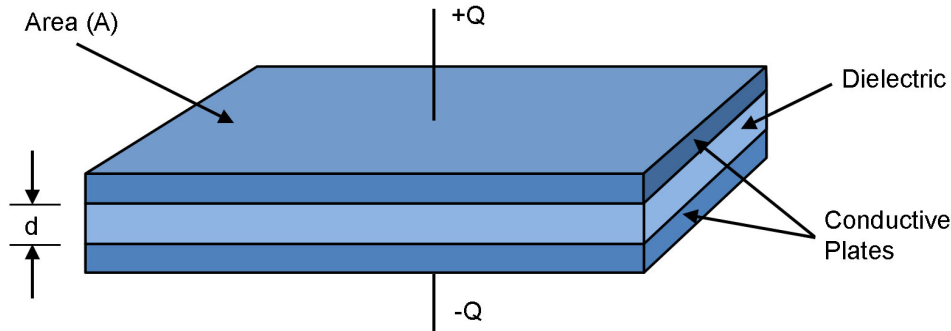


Figure 3.1. Parallel capacitor model with dielectric sandwiched between two conductive plates.

A typical LCR meter measures C as the real part and D as the loss factor of the complex capacitance, where

$$C^*(f) = C(f)[1 - jD(f)]$$

and this means, for the parallel-plate geometry, $C = \varepsilon' A/d$ and $D = \varepsilon''/\varepsilon'$. A typical LCR meter covers frequency range ~ 1 Hz to ~ 1 MHz, although specialized dielectric spectrometers can access ~ 1 MHz to ~ 1 GHz (Novocontrol).^(a) Permittivity measurements up to potentially hundreds of gigahertz can be accessed using waveguide approaches, and at even higher frequencies using optical test methods.

(a) <https://www.novocontrol.de/php/index.php>

3.2 Permittivity of Polymers

The permittivity of any material, measured at a particular frequency, likely involves the sum of several types of dipolar contribution. In polymers, the particular contributions depend on the composition of the material and the frequency of the measurement. The dipolar contributions may be from dipoles induced by the applied electric field or from dipoles permanently present in the material. All materials exhibit electronic polarization that arises as a consequence of relative displacement of electronic and nuclear charge in the presence of an applied electric field. Because the electron cloud is relatively light and responsive to the presence of the applied electric field, this polarization mechanism persists up to $\sim 10^{15}$ Hz. Permanent dipole moments in the polymer itself also contribute to the permittivity of the material. These may be associated with side groups attached to the polymer main chain, or with the polymer main chain itself. Those dipole moments associated with the polymer chain tend to become active in their polarization contribution at temperatures above the glass transition temperature T_g of the polymer, and the observance of this contribution to polarization can indeed be used as a measure of T_g . Contributions from side groups may be observable at temperatures both above and below T_g , with relaxation frequency higher than that of any relaxation associated with the polymer main chain. For further information, see, for example, Menczel and Prime (2009, Chapter 6).

Each dipole has associated with it a polarizability, α , and dipole moment $p = \alpha E$. The extent to which each dipole may contribute to the overall polarization of the material depends on the strength of the individual contribution, represented by its polarizability. The polarizability is a function of frequency, giving rise to frequency dependence of the permittivity. Each type of contribution has a characteristic relaxation frequency associated with it, above which its contribution to the overall polarization of the material falls off. This behavior is illustrated in Figure 3.2, which shows the frequency dependence of permittivity for a typical polymer. Three relaxations are illustrated—interfacial polarization relaxation that can occur when free charges in a semi-crystalline polymer become trapped at the crystal-amorphous boundary, for example; the alpha relaxation associated with the glass transition mentioned before; and a beta relaxation associated with polarization of a side group. The strength of each relaxation and its frequency depends on the particulars of the material. Notice that each relaxation is characterized by a decline in ϵ' and a peak in ϵ'' . These real and imaginary parts of the same complex number are related mathematically by the Kramers-Kronig relations that are rooted in the causal nature of the relaxation process (Landau and Lifshitz 1960).

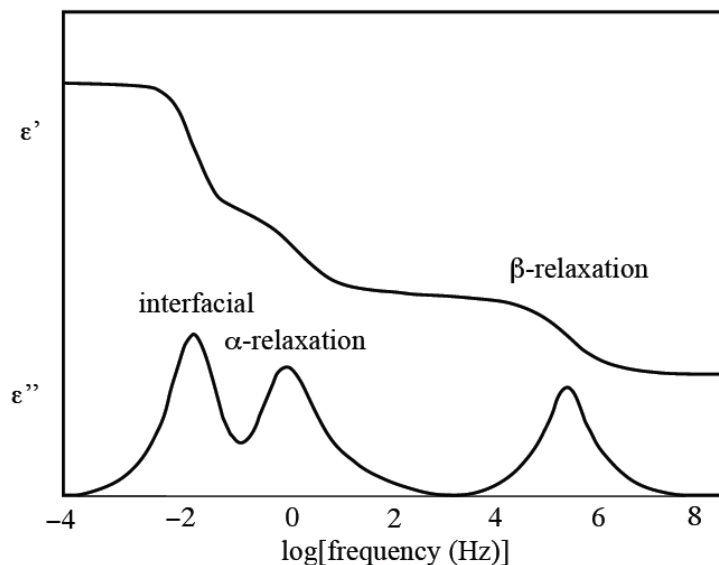


Figure 3.2. Frequency-dependence of ϵ' and ϵ'' for relaxation modes in typical polymers (Bowler and Liu 2015).

3.3 Cable System Capacitance and Impedance

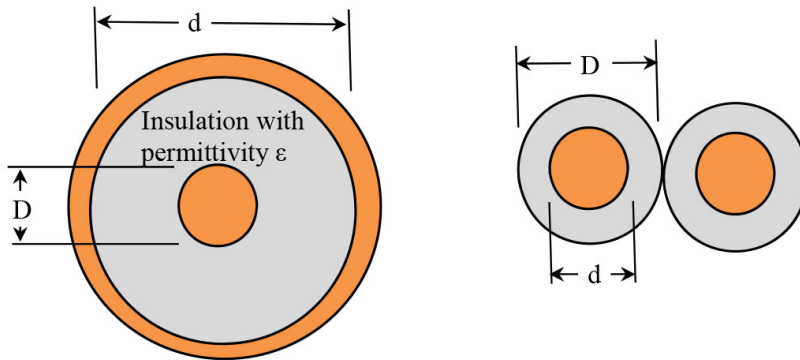
The concept of measuring the capacitance and impedance of a dielectric material can be extended to either co-axial cables or multi-conductor cables by considering the conductors as analogous to the parallel plates. The measured capacitance (C) relation to the insulation permittivity (ϵ pF/ft.) is more complex but the idea is the same. The nominal capacitances and open circuit impedances can be calculated from standard formulas that can be found in reference text books or web pages (Figure 3.3) (Standard Wire & Cable Co. 2009).

Formulas for distributed line capacitance for the two cases illustrated in Figure 3.3 are as follows. For the coaxial line shown in Figure 3.3 left,

$$C_{pF/ft.} = \frac{7.36\epsilon}{\text{Log}\left(\frac{D}{(sf)(d)}\right)}$$

For the two-wire (twisted pair) line shown in Figure 3.3 right,

$$C_{unshielded \frac{pF}{ft.}} = \frac{3.7\epsilon}{\text{Log}\left(\frac{1.2D}{(sf)d}\right)} \quad C_{shielded \frac{pF}{ft.}} = \frac{2.9\epsilon}{\text{Log}\left(\frac{1.5D}{(sf)d}\right)}$$



$C_L = 7.36 * \epsilon / \text{LOG} (D/ [(sf) (d)])$
 For coaxial cable where
 C_L = Capacitance / unit length in pF/ft.
 sf = stranding factor^(a)
 ϵ = dimensionless dielectric constant

$C_L = 3.7 * \epsilon / \text{LOG} ([1.2*D]/ [(sf) (d)])$
 For twisted pair (unshielded) where
 C_L = Capacitance / unit length in pF/ft.
 sf = stranding factor^(a)
 ϵ = dimensionless dielectric constant

(a) Stranding factor is typically provided in the cable specifications and relates to the conductor void space. For a single-strand conductor, the stranding factor is 1.0.

Figure 3.3. Configuration and formulas for calculating nominal cable capacitance (Standard Wire & Cable Co. 2009).

The nominal values of permittivity for any particular insulation material vary substantially as a function of both frequency and insulation polymer age condition. Thus, these design equations are only accurate predictors of cable capacitance or impedance for the specific permittivity of the cable insulation.

Cable systems can be modeled based on these generalizations to appreciate system behavior. One focus of PNNL's previous work has been an appreciation of the influence of a defect profile on measured cable conditions. This concept extends to DS as shown in Figure 3.4. A 36 m section of twisted-pair cable was modeled as a series connection of two 18 m cable segments, and the impedance measurement was simulated with the following conditions:

- Pristine – all segments with nominal capacitance values.
- Both segments aged – all segments with a 20% increase in their parallel capacitance.
- 50% aged – the segment furthest away from the measurement port represented with a 20% increase in the nominal cable capacitance.

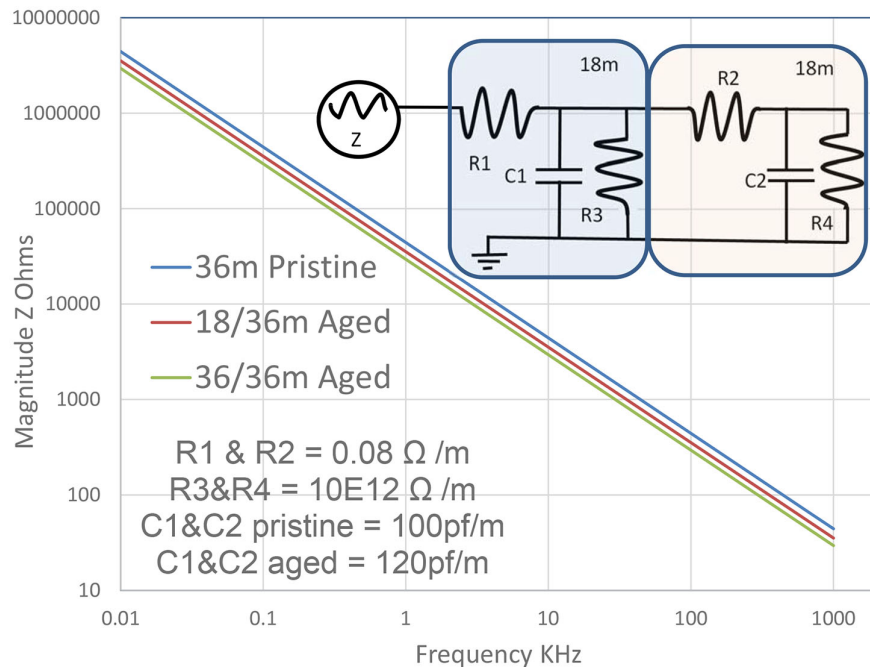


Figure 3.4. Simulated magnitude Z (ohms) plot of pristine, 50% aged, and 100% aged twisted-pair cable based on simple resistance and capacitance series and parallel impedance model.

Note that for this cable, the response is dominated by the capacitance. As the capacitance increases (corresponding to increased aging), the magnitude impedance decreases. Generally, the impedance of the cable will be a proportional average of the percent of unaged or pristine cable and the percent of aged cable. Frequently, the aging profile of the cable is not known, but assuming the cable is uniformly aged along its entire length is a non-conservative assumption.

4. DS MEASUREMENTS ON TRIPLEX (THREE-CONDUCTOR) CABLE

The goal of this work is to assess the ability of DS to distinguish between a pristine three-conductor cable and a similar cable containing a thermally-aged center section.

Prior work has demonstrated the usefulness of DS conducted on intact cables for cable insulation assessment (Verardi 2013; Linde et al. 2015; Imperatore 2017; Imperatore et al. 2017).

4.1 Cable Sample Preparation

4.1.1 Cable

The cable selected for study is of the following type: General Cable FR-EPR/CPE, Instrumentation, Shielded 600 V, UL Type TC, Overall Shielded Triad (Figure 4.1).

The cable dimensions are provided in Table 4-1 and details of the materials used in its construction are provided below.

- **Conductor:** 16 AWG tinned, annealed copper
- **Insulation:** Flame Retardant Ethylene Propylene Rubber (EPR) Type II (color-coded per ICEA Method 1: triad - black, white and red)
- **Shield:** Flexfoil® aluminium/polymer in contact with stranded tinned copper drain wire
- **Jacket:** Lead-free, flame-retardant, thermoplastic chlorinated polyethylene (CPE)

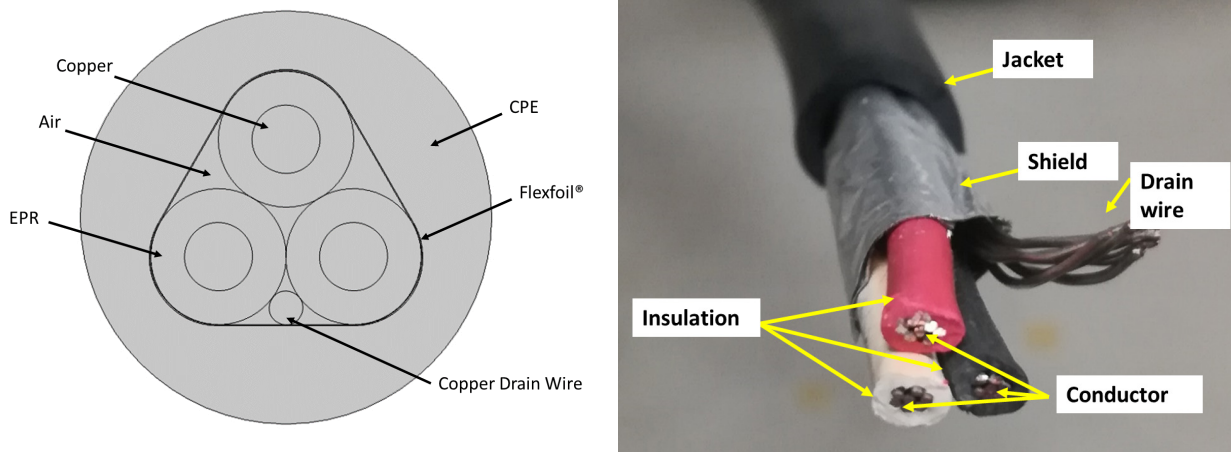


Figure 4.1. Cross-section schematic of the cable (*left*) and photograph (*right*).

Table 4-1. Cable dimensions.

Cond. Size (AWG)	Cond. Size (mm)	Cond. Strand	Minimum Avg. Insulation Thickness (mm)	Minimum Avg. Jacket Thickness (mm)	Nominal Cable Outer Diameter (mm)
16	1.291	7W	0.64	1.14	8.51

4.1.2 Samples

Pristine samples (1, 2, and 3) were made available in three different lengths, summarized in Table 4-2 and shown in Figure 4.2. An aged sample was prepared by enclosing a 90.2 cm long center section of a 3024 cm long cable in an air-circulating oven and aging the enclosed section for 1,600 h at 140°C (Figure 4.3). In the 90.2 cm long aged section, approximately 48% of the cable surface area showed loss of jacket (only) after aging and approximately 7% of the cable surface area showed loss of jacket and shield.

Table 4-2. Sample specifications.

Sample #	Aging	Length (cm)
1	No	9.5 ± 0.1
2	No	47.7 ± 0.1
3	No	308 ± 0.1
Aged	Yes	3024 ± 0.1

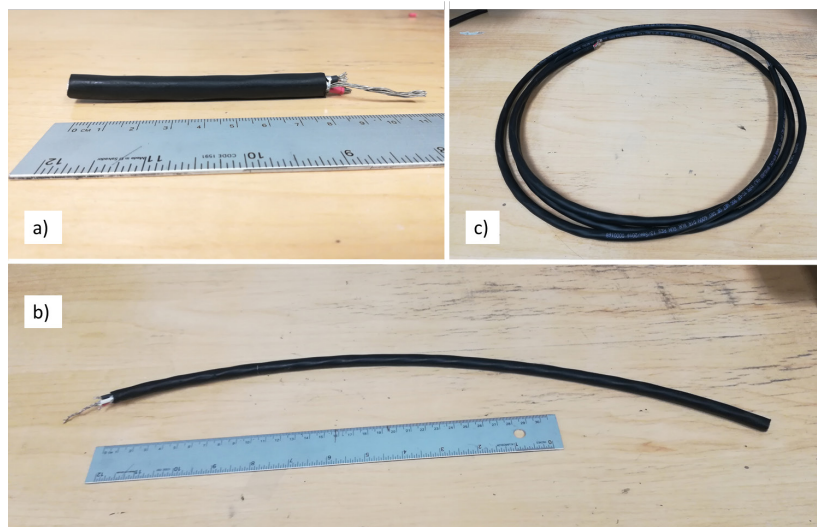


Figure 4.2. Pristine samples with length 9.5 cm (a), 47.7 cm (b), and 308 cm (c).



Figure 4.3. Cable with aged section: aging setup (*left*) and photograph of the aged cable section showing loss of jacket and shield in places (*center and right*). Grid is 1 cm.

4.2 DS Measurement Method

4.2.1 Experiment Procedure

Capacitance was measured using an Agilent E4980A Precision LCR Meter with a two-point 16095A probe test fixture. An open-short calibration procedure was conducted prior to sample measurement. Electrical contact was made with the sample via the 16095A probe test fixture and a potential difference of 1 V applied to the sample with the black-insulated conductor being held at +1 V and the other two conductors plus the shield being held at 0 V (Figure 4.4). Frequency was swept from 2 Hz to 2 MHz, yielding a useful range of 100 Hz to 100 kHz, outside of which uncertainties were unacceptably large. Eight data sets were recorded for each pristine sample, and five data sets were recorded for each sample taken from the aged cable. Each data set was recorded using a moving average with factor 8.

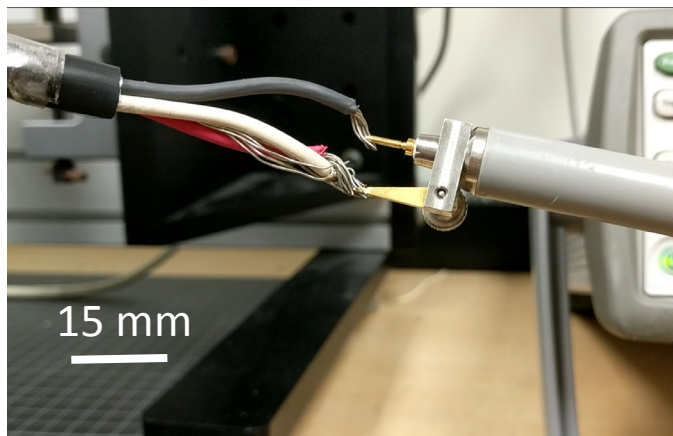


Figure 4.4. Agilent two-point 16095A probe text fixture in contact with cable sample.

4.2.2 Experiment Sequence

1. Dielectric spectroscopy has been conducted on the pristine cables (samples 1, 2, and 3), obtaining a plot of the complex capacitance versus frequency. Then, using these capacitance values as inputs to a COMSOL™ model, the correct value for ϵ_{EPR} for each value of frequency has been inferred. Values of CPE permittivity are not needed as inputs to the model, because the cable is shielded and thus the electric field does not interact with the CPE jacket.
2. Dielectric spectroscopy was conducted on the aged cable, starting with the original length, then cutting off a section of a certain length (Table 4-3) and repeating DS on the remaining portion, then repeating until the last measurement is made on the aged section only. The choice of cable length for removal with each cut was made to give a range of values of the R defined as follows

$$R(\%) = \frac{\text{Length of thermally aged section}}{\text{Total length of cable section}} \times 100.$$

3. Dielectric spectroscopy was conducted on the aged section that remains after all unaged material has been cut from the sample.
4. Permittivity was inferred by COMSOL™ from measurements on the pristine cable.
5. R was evaluated and results plotted as a function of R. A linear fit was made to the measured C and D.
6. Sectioned portions of the aged cable were tested to look for any effect of proximity to the aged section.

7. Specific C and D were measured on sectioned portions of pristine cable and compared to look for any effect of cable length on the data.
8. Measurements were made on a pristine cable section (1 m) with successive portions of removed jacket and shield to investigate the effect of jacket/shield loss observed in the aged section.

Table 4-3. Sample section lengths, aged cable. Samples AP1 and AP8 were at each end of the original cable; whereas, AP7 and AP14 were adjacent to the aged section, as in the order listed in the table.

Sample	Length (m)	Sample	Length (m)
AP1	4.617	AP14	0.221
AP2	7.284	AP13	0.583
AP3	3.823	AP12	0.583
AP4	1.812	AP11	1.116
AP5	0.861	AP10	2.582
AP6	0.610	AP9	2.588
AP7	0.288	AP8	2.295
Aged	0.902		

4.3 Results and Discussion

Absolute capacitance values measured on the pristine samples are plotted in Figure 4.5, where the linear influence of sample length is clear. All data sets plotted are the average of eight distinct trials, each of which was recorded using a moving average with factor 8.

Insulation permittivity (real part) is presented in Figure 4.6 for pristine samples of different lengths and was inferred from the capacitance data presented in Figure 4.5 by COMSOL™ simulation. The real relative permittivity of the insulation in the pristine samples agrees closely from sample to sample.

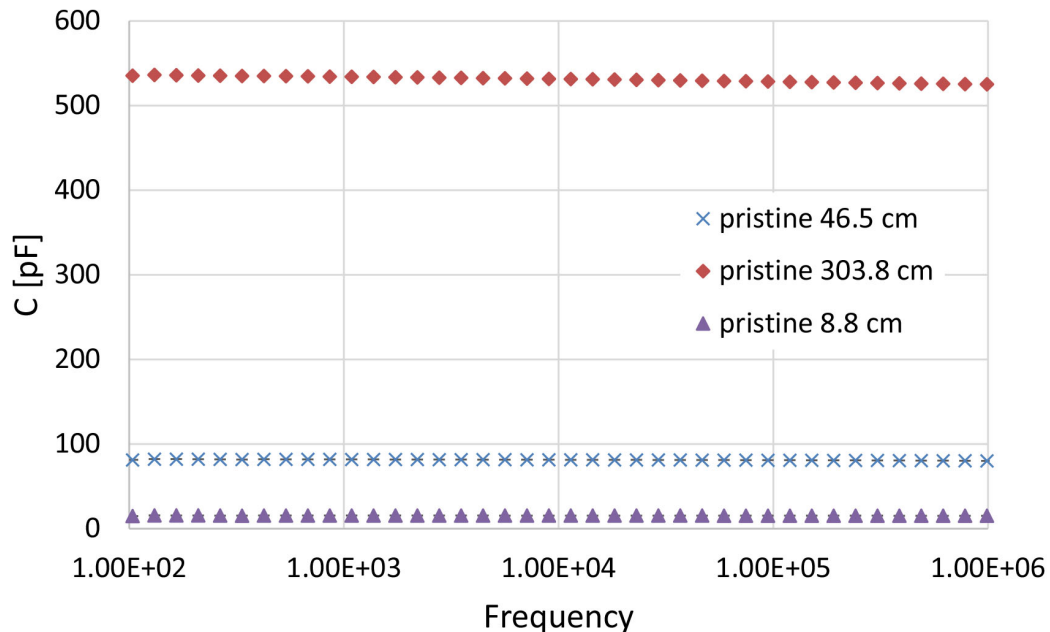


Figure 4.5. Absolute capacitance measured on pristine samples.

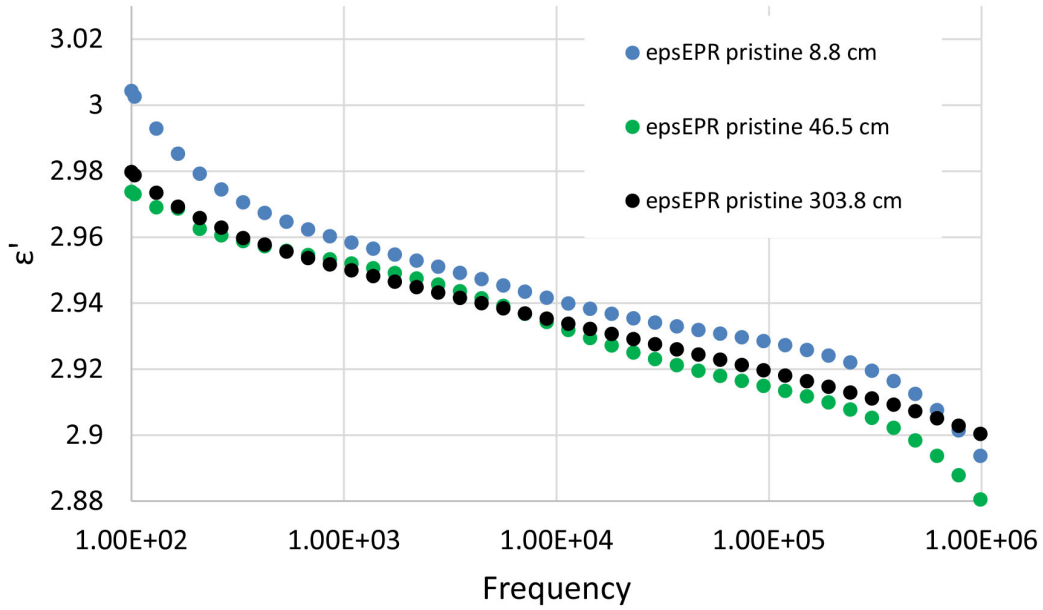


Figure 4.6. Insulation real relative permittivity inferred from capacitance data shown in Figure 4.5, measured on pristine samples of different length, by COMSOL™ simulation.

Distributed capacitance measured upon aged samples with various values of R are shown in Figure 4.7. The ‘damage ratio’ R indicates the percentage of aged cable compared to the total sample length, for the aged sample, Table 4-2. The capacitance is presented as specific capacitance (pF/m) i.e., normalized by length. Distributed dissipation factor for the same sample is shown in Figure 4.8. Symbols represent the average of five trials and error bars represent one standard deviation of that data. Results are similar regardless of which end of the sample (A or B) is connected to the instrument. The concept of damage ratio (R) is more fully explored in (Gagliani 2018).

A linear fit to the measured distributed capacitance data can be made in general:

$$C_R = \frac{(C_{100} - C_0)}{100} R + C_0$$

where C_R represents the distributed capacitance measured for a particular R and, in this particular case, $C_R = 0.690R + 187$ pF/m with confidence $R^2 = 0.9975$ for frequency 1.02 kHz. Note, the value of measured capacitance for $R = 100\%$, i.e., measured on the fully aged section, gave rise to a value of C lower than expected from the linear trend. This behavior is likely due to partial loss of shield and jacket from the aged section, as shown in Figure 4.7 and investigated in detail below. Similarly, a linear fit to the dissipation data can be made in general:

$$D_R = \frac{(D_{100} - D_0)}{100} R + D_0$$

and, in this particular case, $D_R = 0.690R + 0.00336$ with confidence $R^2 = 0.9795$ for frequency 1.02 kHz.

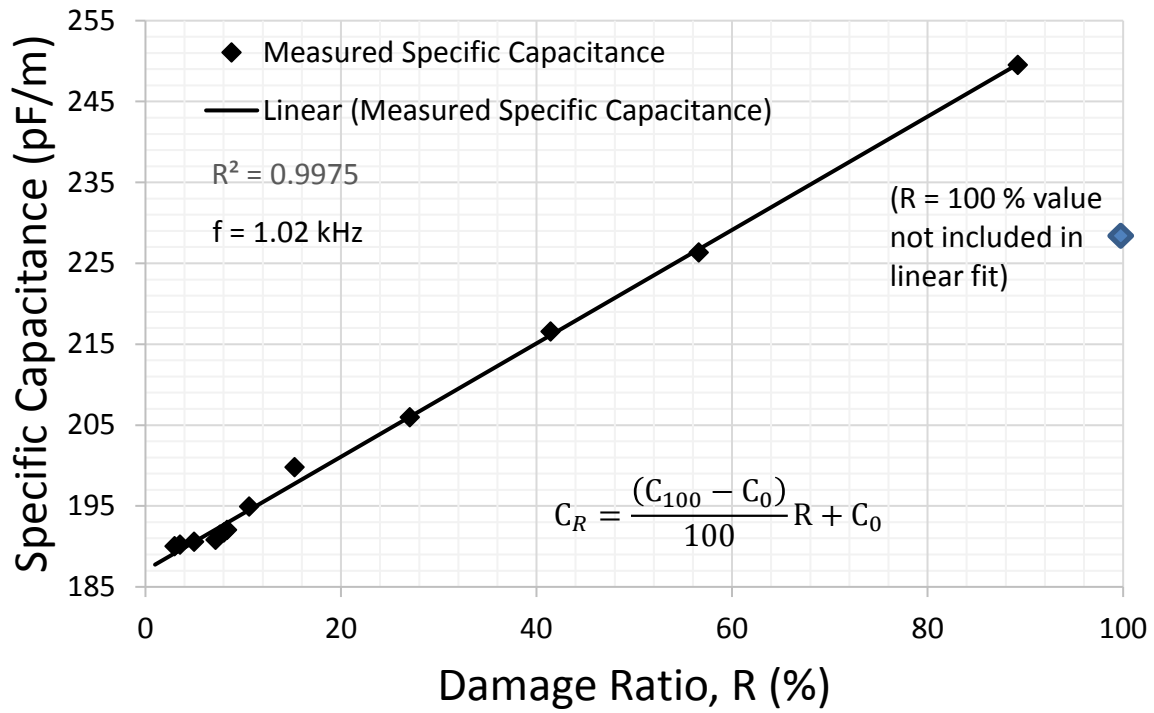


Figure 4.7. Specific capacitance (distributed) measured on samples with various values of R.

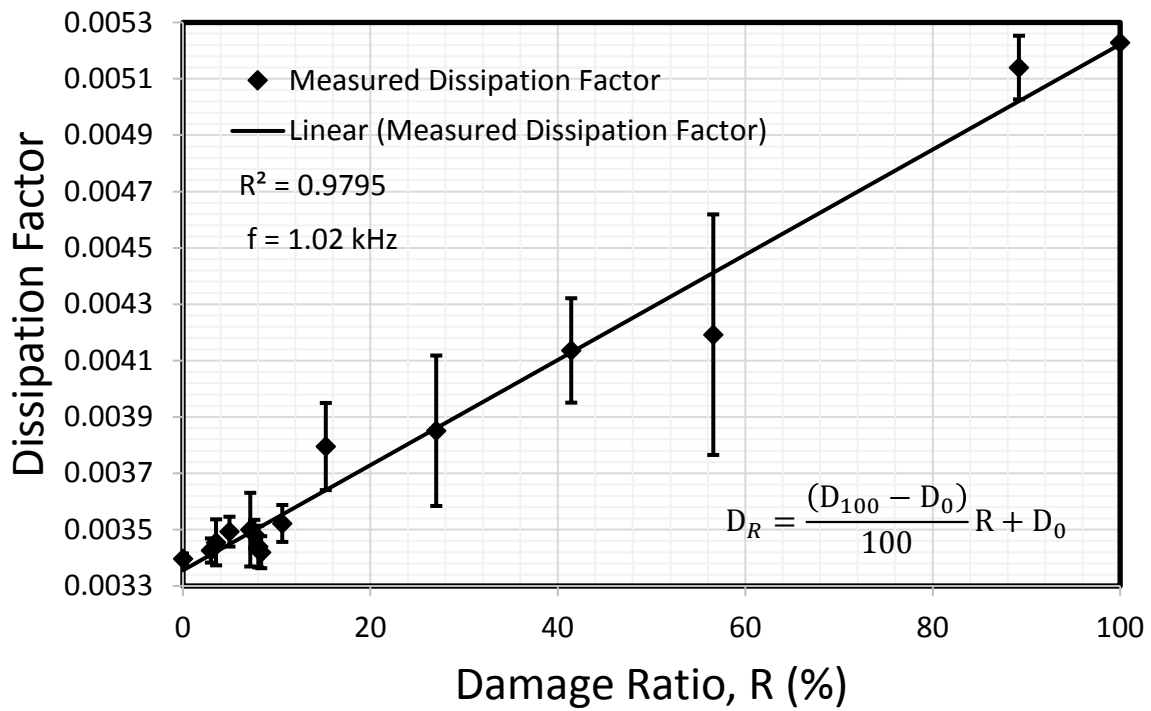


Figure 4.8. Dissipation factor (distributed) measured on samples with varying values of R.

The effect of proximity to the oven on the cable as it aged was investigated by measuring distributed C and D on all the sections listed in Table 4-3. Specific C is plotted in Figure 4.7 and D in Figure 4.8, for frequency 1.02 kHz, as a function of the distance of each section center from the center of the aged section. In both cases it is observed that there is no significant trend in C or D as a function of distance of the sample section from the aged section.

The effect of sample length on measured specific C and D was investigated and the results are shown in Figure 4.9 and Figure 4.10. It can be seen that there is no significant trend associated with sample length, as should be the case.

The effect of lost jacket and/or shield on measured C was investigated by removing the jacket alone from a 100 cm long pristine cable sample in 10% increments and jacket plus shield in 10% from another 100 cm long pristine cable sample in 10% increments, collecting data as each increment was removed. The results are shown in Figure 4.11 for frequency 1.02 kHz. It can be seen that removing the jacket alone results in a linear reduction in specific capacitance at a rate of -0.307 pF/m/cm. The effect of removing both jacket and shield results in a stronger linear reduction of specific capacitance, at a rate of -1.14 pF/m/cm. This observed behavior provides support for the hypothesis that the significant reduction observed in C_{100} compared with the value expected from the linear trend observed in Figure 4.12 is due to loss of jacket and shield (Figure 4.13).

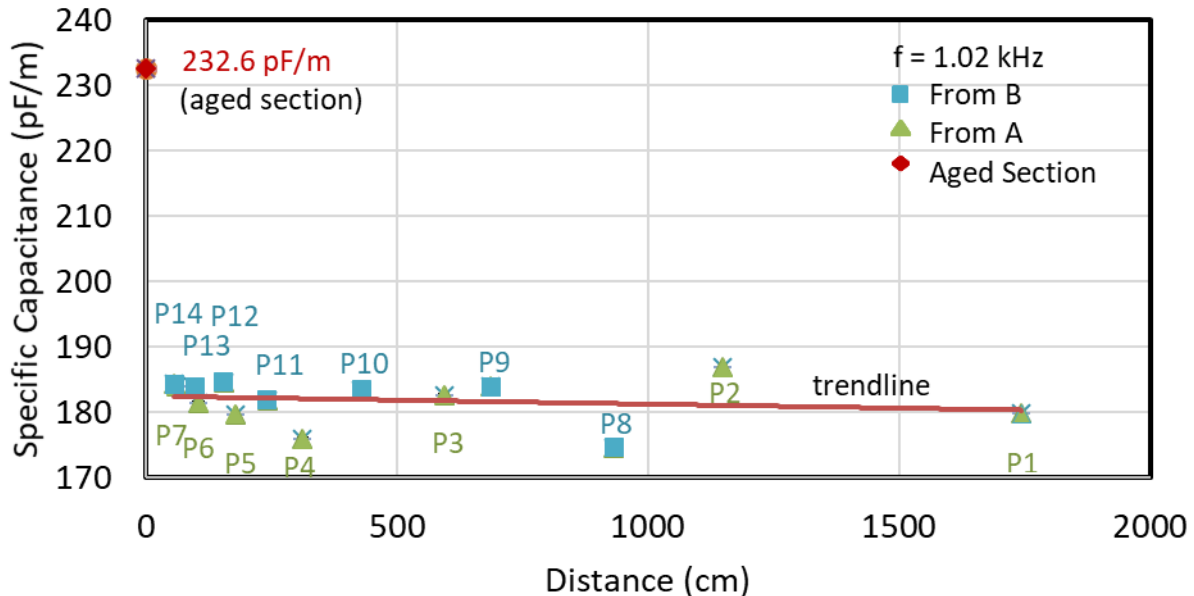


Figure 4.9. Specific capacitance measured on samples with various lengths (Table 4-3) plotted as a function of distance from aged cable section

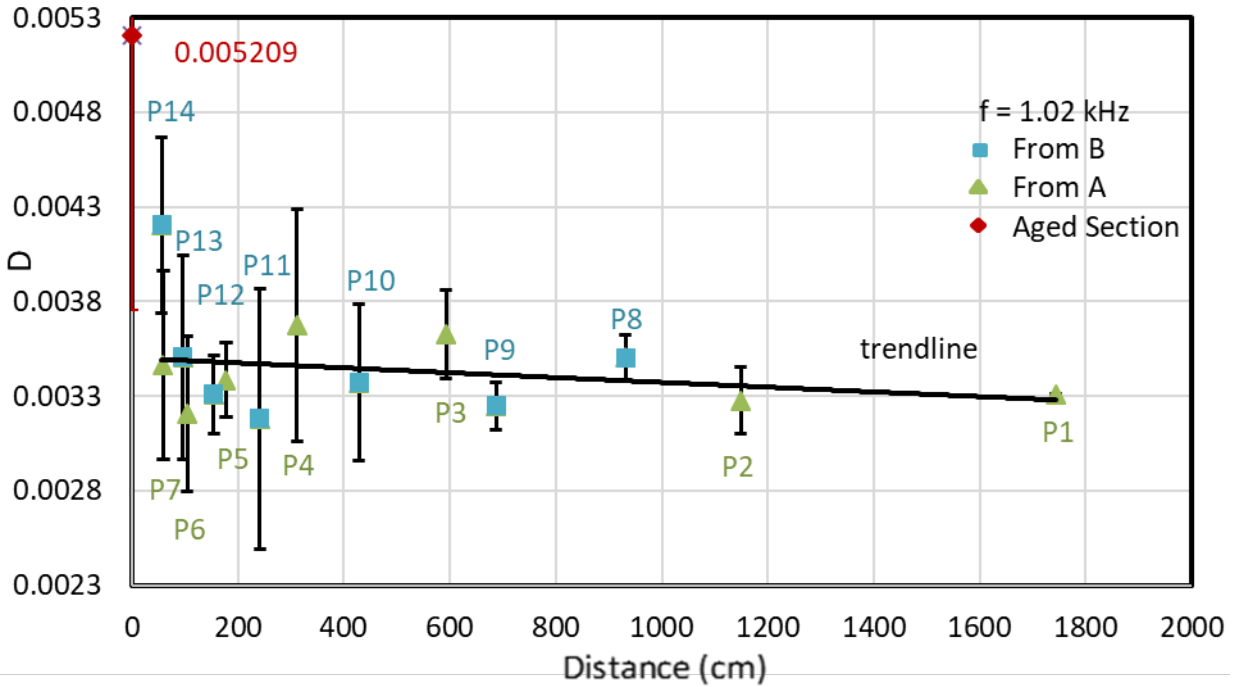


Figure 4.10. Dissipation factor measured on samples with various lengths (Table 4-3) plotted as a function of distance from the aged cable section.

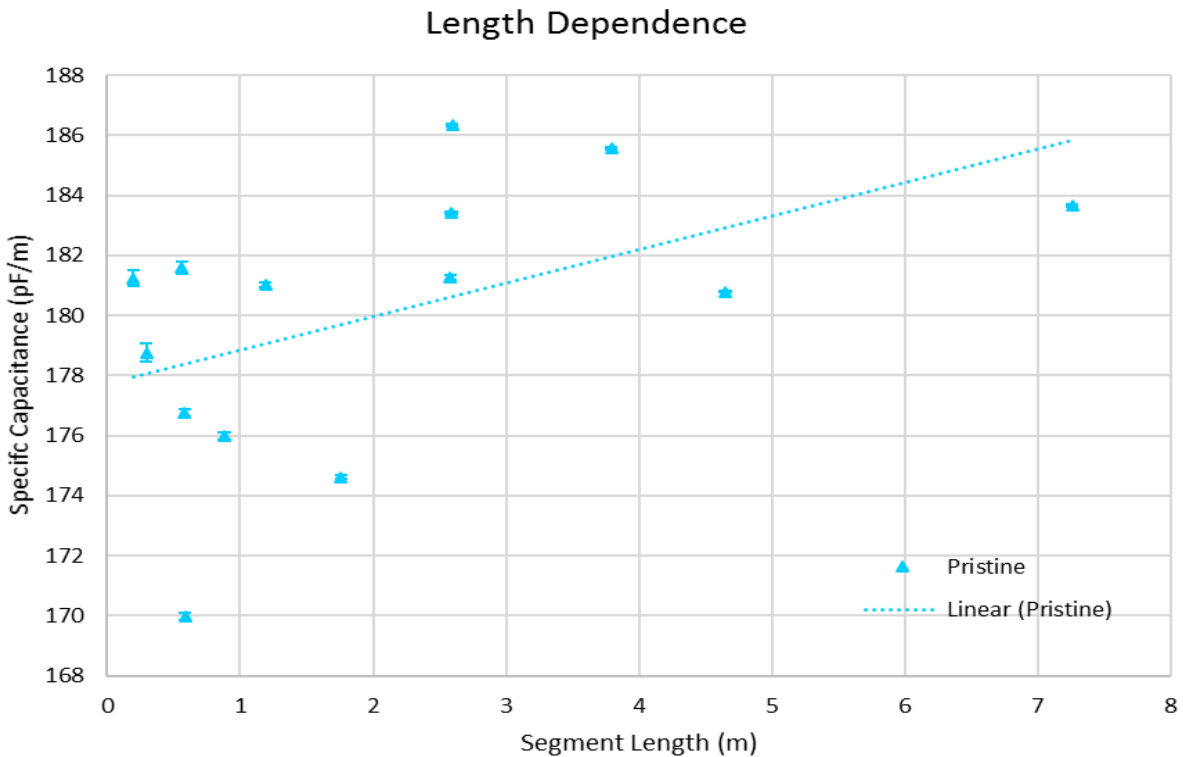


Figure 4.11. Specific capacitance (distributed) measured on pristine samples with various lengths plotted as a function of sample (segment) length for frequency 1.02 kHz.

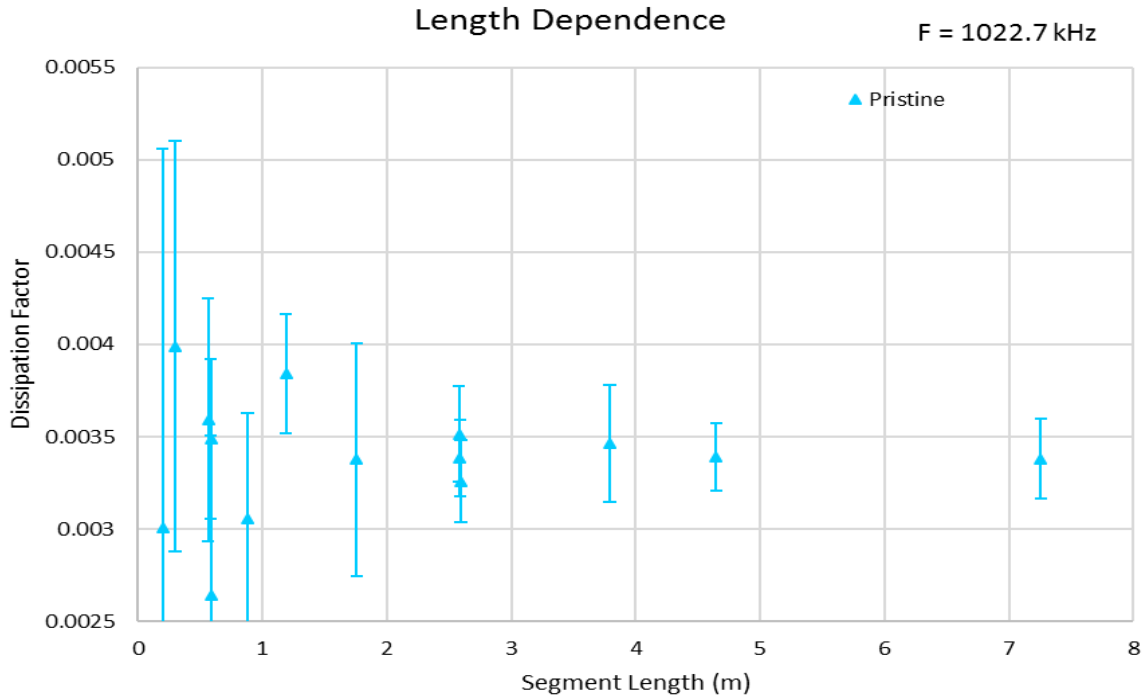


Figure 4.12. Dissipation factor measured on pristine samples with various lengths plotted as a function of sample (segment) length for frequency 1.02 kHz.

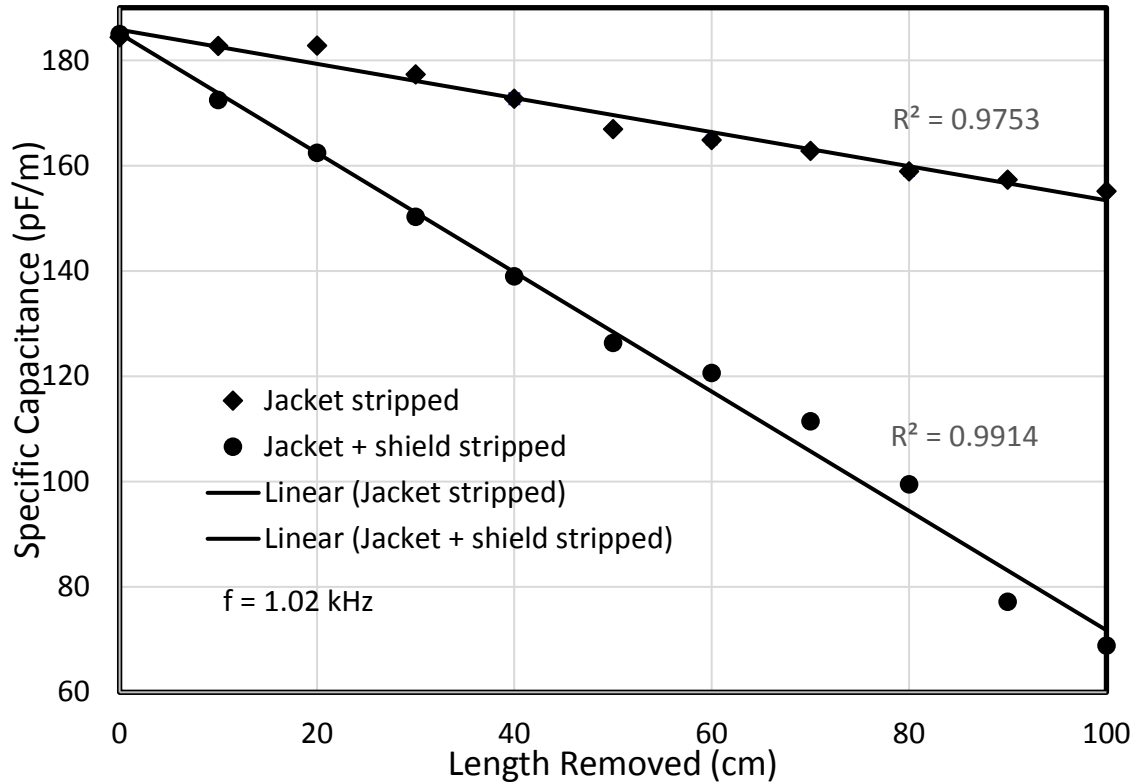


Figure 4.13. Specific capacitance (distributed) measured on 100 cm long pristine samples as a function of the length of removed jacket or jacket and shield.

5. CONCLUSIONS

Conclusions and observations are as follows:

- A substantial body of work suggests feasibility to measure cable insulation conditions using various forms of DS.
- Measured specific capacitance and dissipation factor:
 1. increases significantly with thermal aging of flame-resistant EPR/CPE shielded triad instrumentation cable (General Cable) due to material property changes
 2. increases linearly with increasing damage ratio in a cable.
- Specific capacitance:
 1. decreases linearly with increasing area of removed cable jacket and/or shield
 2. C decreases to a relatively larger degree when both jacket and shield are removed.
- The thermally aged section of the cable significantly increases capacitance values even at low R.
- Dissipation factor shows the same increasing trend with damage ratio and to a relatively larger degree.
- The DS measurement represents an average of the dielectric condition over the entire cable. If only a small percentage of the cable is damaged, this should be considered when assessing the DS measurement. An assumption that the damage is distributed along the entire cable length is a non-conservative assumption.

6. PLANS FOR CONTINUED WORK

- Modeling work may be extended to consider actual permittivity spectral responses and further examine the influence of damage profile.

7. REFERENCES

- Bowler N and S Liu. 2015. "Aging Mechanisms and Monitoring of Cable Polymers." *International Journal of Prognostics and Health Management* 6.
https://www.phmsociety.org/sites/phmsociety.org/files/phm_submission/2015/ijphm_15_029.pdf.
- Brown J, R Bernstein, G Von White II, S Glover, J Neely, G Pena, K Williamson, F Zutavem and F Gelbard. 2015. *Submerged Medium Voltage Cable Systems at Nuclear Power Plants: A Review of Research Efforts Relevant to Aging Mechanisms and Condition Monitoring*. SAND2015--1794. Albuquerque, NM: Sandia National Laboratories. DOI: 10.2172/1177756.
- Chen T and N Bowler. 2009. "Analysis of Concentric Coplanar Capacitor for Quantitative Dielectrometry." In *Studies in Applied Electromagnetics and Mechanics, Vol. 33: Electromagnetic Nondestructive Evaluation (XIII)*, pp. 61-68. eds: JS Knopp, MP Blodgett, B Wincheski and N Bowler. The Netherlands: IOS Press. DOI: 10.3233/978-1-60750-554-9-61.
- Chen T and N Bowler. 2013. "Design of Interdigital and Concentric Capacitive Sensors for Materials Evaluation." In *Proceedings of the 39th Annual Review of Progress in Quantitative Nondestructive Evaluation*, pp. 1593-1600. July 15-20, 2012, Denver, CO. American Institute of Physics, Melville, NY. AIP Vol. 1511.
- EPRI. 2005. *Initial Acceptance Criteria Concepts and Data for Assessing Longevity of Low-Voltage Cable Insulations and Jackets*. TR-1008211. Palo Alto, CA: Electric Power Research Institute (EPRI).
- EPRI. 2015. *Plant Engineering: Evaluation and Insights from Nuclear Power Plant Tan Delta Testing and Data Analysis - Update*. TR-3002005321. Palo Alto, CA: Electric Power Research Institute.
- EPRI. 2017. *Long-Term Operations: Initial Findings on Use of Dielectric Spectroscopy for Condition Monitoring of Low Voltage Nuclear Power Plant Cables*. TR-3002010403. Palo Alto, CA: Electric Power Research Institute.
- European Commission. 2014. *Final Report Summary - ADVANCE (Ageing Diagnostics and Prognostics of Low-Voltage I&C Cables)*. Project ID: 269893. France: Electricite de France, S.D. Available at https://cordis.europa.eu/result/rcn/149266_en.html.
- Fifield LS, MP Westman, A Zwoster and B Schwenzer. 2015. *Assessment of Cable Aging Equipment, Status of Acquired Materials, and Experimental Matrix at the Pacific Northwest National Laboratory*. PNNL-24198. Richland, WA: Pacific Northwest National Laboratory.
- Gagliani R. 2018. *Distributed Capacitance Sensing for Characterization of Nuclear Power Plant Cables*. Masters Thesis, University of Bologna, Bologna, Italy. Available at <https://amslaurea.unibo.it/17155/#>.
- Glass SW, LS Fifield, N Bowler, A Sriraman and WC Palmer. 2018a. *Interdigital Capacitance Local Non-Destructive Examination of Nuclear Power Plant Cable for Aging Management Programs*. PNNL-27546. Richland, WA: Pacific Northwest National Laboratory.
- Glass SW, LS Fifield, G Dib, JR Tedeschi, AM Jones and TS Hartman. 2015. *State of the Art Assessment of NDE Techniques for Aging Cable Management in Nuclear Power Plants FY2015*. M2LW-15OR0404024, PNNL-24649. Richland, WA: Pacific Northwest National Laboratory.
- Glass SW, LS Fifield and TS Hartman. 2016. *Evaluation of Localized Cable Test Methods for Nuclear Power Plant Cable Aging Management Programs*. M3LW-16OR0404022, PNNL-25432. Richland, WA: Pacific Northwest National Laboratory.

Glass SW, AM Jones, LS Fifield, N Bowler, R Gagliani and A Sriraman. 2018b. *Dielectric Spectroscopy for Bulk Condition Assessment of Low Voltage Cable -- Interim Report*. PNNL-27982. Richland, WA: Pacific Northwest National Laboratory.

Glass SW, AM Jones, LS Fifield, TS Hartman and N Bowler. 2017. *Physics-Based Modeling of Cable Insulation Conditions for Frequency Domain Reflectometry (FDR)*. PNNL-26493. Richland, WA: Pacific Northwest National Laboratory.

IAEA. 2017. *Benchmark Analysis for Condition Monitoring Test Techniques of Aged Low Voltage Cables in Nuclear Power Plants: Final Results of a Coordinated Research Project*. IAEA-TECDOC-1825. Vienna, Austria: International Atomic Energy Agency (IAEA). Available at <https://www-pub.iaea.org/MTCD/Publications/PDF/TE-1825web.pdf>.

Imperatore MV. 2017. *Dielectric Spectroscopy as a Condition Monitoring Diagnostic Technique for Thermally Aged PVC/EPR Nuclear Power Plant Cables*. Masters Thesis, University of Bologna, Italy.

Imperatore MV, LS Fifield, D Fabiani and N Bowler. 2017. "Dielectric Spectroscopy on Thermally Aged, Intact, Poly-vinyl Chloride/Ethylene Propylene Rubber (PVC/EPR), Multipolar Cables." In *2017 IEEE Conference on Electrical Insulation and Dielectric Phenomena (CEIDP)*, pp. 173-176. October 22-25, 2017, Fort Worth, TX. DOI: 10.1109/CEIDP.2017.8257522. IEEE.

Kremer F and A Schonhals. 2003. *Broadband Dielectric Spectroscopy*, Berlin: Springer.

Landau LD and EM Lifshitz. 1960. *Mechanics, Third Edition, Volume 1 of Course of Theoretical Physics*, Oxford: Butterworth Heinemann.

Linde E, L Verardi, D Fabiani and UW Gedde. 2015. "Dielectric Spectroscopy as a Condition Monitoring Technique for Cable Insulation Based on Crosslinked Polyethylene." *Polymer Testing* 44:135-142. DOI: 10.1016/j.polymertesting.2015.04.004.

Mantey A. 2015. "Evaluation and Insights from Nuclear Power Plant Tan Delta Testing and Data Analysis-Update." Presented at *Power and Energy Society Insulated Conductors Committee, Subcommittee D*, November 3, 2015, Tucson, AZ.

Menczel JD and RB Prime, Eds. 2009. *Thermal Analysis of Polymers: Fundamentals and Applications*. Hoboken, NJ: Wiley. ISBN 978-0-471-76917-0.

Nassr AA and WW El-Dakhkhni. 2009. "Non-destructive Evaluation of Laminated Composite Plates Using Dielectrometry Sensors." *Smart Materials and Structures* 18(5):055014. DOI: 10.1088/0964-1726/18/5/055014.

NRC. 2012. *Condition-Monitoring Techniques for Electric Cables Used in Nuclear Power Plants*. Regulatory Guide 1.218. Washington, D.C.: U.S. Nuclear Regulatory Commission. Available at <http://pbadupws.nrc.gov/docs/ML1035/ML103510447.pdf>. ADAMS Accession No. ML103510447.

Ramuhalli P, LS Fifield, MS Prowant, G Dib, JR Tedeschi, JD Suter, AM Jones, MS Good, SW Glass and AF Pardini. 2015. *Assessment of Additional Key Indicators of Aging Cables in Nuclear Power Plants -- Interim Status for FY2015*. PNNL-24309. Richland, WA: Pacific Northwest National Laboratory.

Rogovin D and R Lofaro. 2006. *Evaluation of the Broadband Impedance Spectroscopy Prognostic/Diagnostic Technique for Electric Cables Used in Nuclear Power Plants*. NUREG/CR-6904; BNL-NUREG-75208-2005. Washington, D.C.: U.S. Nuclear Regulatory Commission. Available at <http://www.nrc.gov/reading-rm/doc-collections/nuregs/contract/cr6904/cr6904.pdf>.

Sheldon RT and N Bowler. 2014a. "Dielectrometry Sensors for Nondestructive Testing of Glass-fiber Polymer-matrix Composites." *Materials Evaluation* 72(11):1421-1427.

Sheldon RT and N Bowler. 2014b. "An Interdigital Capacitive Sensor for Nondestructive Evaluation of Wire Insulation." *IEEE Sensors Journal* 14(4):961-970. DOI: 10.1109/JSEN.2014.2301293.

Simmons KL, LS Fifield, MP Westman, JR Tedeschi, AM Jones, MS Prowant, AF Pardini and P Ramuhalli. 2014. *Determining Remaining Useful Life of Aging Cables in Nuclear Power Plants -- Interim Status for FY2014*. PNNL-23624; INL-EXT-14-32505 Rev. 0. Richland, WA: Pacific Northwest National Laboratory.

Simmons KL, P Ramuhalli, DL Brenchley and JB Coble. 2012. *Light Water Reactor Sustainability (LWRS) Program – Non-Destructive Evaluation (NDE) R&D Roadmap for Determining Remaining Useful Life of Aging Cables in Nuclear Power Plants*. PNNL-21731. Richland, WA: Pacific Northwest National Laboratory.

Standard Wire & Cable Co. 2009. *Cable Design Equations*. Rancho Dominguez, CA: Standard Wire & Cable Co. Available at http://www.standard-wire.com/cable_design_equations.html.

Toman G. 2011. *Plant Engineering: Electrical Cable Test Applicability Matrix for Nuclear Power Plants*. Final Report 1022969. Palo Alto, CA: Electric Power Research Institute.

Verardi L. 2013. *Aging of Nuclear Power Plant Cables: In Search of Nondestructive Diagnostic Quantities*. Ph.D. Thesis, University of Bologna, Italy. Available at <http://amsdottorato.unibo.it/6246/>.

Werelius P, P Tharning, R Eriksson, B Holmgren and U Gafvert. 2001. "Dielectric Spectroscopy for Diagnosis of Water Tree Deterioration in XLPE Cables." *IEEE Transactions on Dielectrics and Electrical Insulation* 8(1):27-42. DOI: 10.1109/94.910423.